



Politecnico
di Bari

Repository Istituzionale dei Prodotti della Ricerca del Politecnico di Bari

Surface and bulk hydrophobic cement composites by tyre rubber addition

This is a post print of the following article

Original Citation:

Surface and bulk hydrophobic cement composites by tyre rubber addition / Di Mundo, R.; Petrella, A.; Notarnicola, M.. - In: CONSTRUCTION AND BUILDING MATERIALS. - ISSN 0950-0618. - ELETTRONICO. - 172:(2018), pp. 176-184. [10.1016/j.conbuildmat.2018.03.233]

Availability:

This version is available at <http://hdl.handle.net/11589/126357> since: 2021-03-06

Published version

DOI:10.1016/j.conbuildmat.2018.03.233

Publisher:

Terms of use:

(Article begins on next page)

Surface and bulk hydrophobic cement composites by tyre rubber addition

Rosa Di Mundo, Andrea Petrella, Michele Notarnicola

*Department of Civil, Environmental, Land, Building Engineering and Chemistry
(DICATECh)*

Politecnico di Bari, via Orabona 4, 70126 Bari, Italy

Corresponding author: rosa.dimundo@poliba.it

Abstract

Penetration of water in cement composites, porous and hydrophilic materials, is cause of progressive deterioration and failure. Standard procedures for protecting building structures generally involve uniquely the modification of the surface by coating or impregnation procedures.

In this work, the addition of tyre rubber (TR) to the cement paste is demonstrated to be effective for developing mortars with a pronounced hydrophobic behavior in every part of their structure. Hydrophobic performances are better in the case of finer TR grains size and for larger TR volume addition. TR mortars show higher porosity than the conventional ones, nevertheless the effect of the low rubber surface energy prevails, and the absorption of water drops is almost completely abated. These lightweight materials result to be very competitive for non-structural applications in agreement with the environmentally sustainable policies finalized to convert a synthetic waste to an engineering resource.

Keywords: waste tyre; rubber; cement composites; mortar; hydrophobic; water absorption; water contact angle; adhesion; porosity

1. Introduction

The increasing number of vehicles on the roads of industrialised and developing nations generates millions of end-of-life (ELT) tyres (about 1.4 billion tyres are sold worldwide every year) which are a large and problematic source of waste, due to the large volume and long durability. The limited space and their potential for reuse has led many countries to impose a ban on the practice of landfilling. The estimated EU annual cost for the management of ELTs is estimated at € 600 million [1-2].

Tyre rubber is resistant to mould, heat humidity, bacterial development, ultraviolet rays, some oils, many chemicals. These characteristics, which are beneficial during on-road life, are disadvantageous in post-consumer life and boost the transformation of this material from an environmental problem to engineering resource.

One of the recovery routes involves the so called “granulate recovery” which involves tyre shredding and chipping, by which tyres are cut into small pieces of different sizes (shreds: 460-25 mm; chips: 76-13 mm; crumb rubber: 5-0.1 mm) [1]. After the removal of the steel and fabric components, the *recycled tyre rubber* (RTR) can be used for a variety of civil engineering applications such as, i.e., soft flooring for playgrounds and sports stadiums, modifier in asphalt paving mixtures or additive/aggregate to cement concrete. Among these, the addition (as crumb rubber) to asphalt mixtures is highly diffused due to the good chemical interaction, even leading to a partial dissolution [3-4].

The recovery of RTR as aggregate in cement structures has been proposed since the 90's but it is considered not convincing compared to applications in asphalt pavements [3,5]. An important reason is the not favorable interaction with the matrix. Indeed, the cement paste is mainly characterized by hydrated metal /semimetal oxides, which explains the hydrophilic nature (high surface energy) of this matrix and the good adhesion to the conventional aggregates generally based on quartz and/or limestone. Rubber, instead, made of organic polymers, is characterized by a low surface energy, and therefore by a hydrophobic character. The interaction hydrophilic-hydrophobic is very unfavorable resulting in a poor adhesion between rubber particles and the

57 cement matrix. Various rubber chemical treatments have been lately tested with the purpose of
58 improving adhesion. Among these, treatments with NaOH [6-8], HNO₃ and cellulosic
59 derivatives [9] or silane coupling agents [10] have been reported.

60 More importantly, lower compression resistances are always observed in rubber-cement
61 composites with respect to the conventional ones [5,11]. This is mainly due to the fact that
62 rubber sites are significantly softer than their surrounding media acting like “holes” inside the
63 concrete. For this reason only non-structural applications have been proposed (exterior wall
64 materials [12], pedestrian blocks, highway sound walls, residential drive ways, and garage
65 floors [3]) and no building practice seems to be diffused.

66 However, an enhancement of toughness and ability to absorb impact energy has been observed
67 (somewhere also explained and modeled), also in addition to an increased flexural strength
68 [3,11].

69 Further, the lightweight character of the rubberized materials (due to the low specific weight of
70 rubber) should be considered an advantage for the use as construction material since nowadays
71 the structural efficiency is more important than the absolute strength level. Specifically, a
72 decreased density for the same strength reduce the dead load, foundation size, and construction
73 costs; it also enhances sound and thermal insulation [13].

74 Our objective is to focus on a specific feature of the rubber–cement composites, i.e. the low
75 surface energy of the rubber particles which, although responsible of a low adhesion to the
76 cement paste, should inhibit the absorption of water in artifacts.

77 This is a relevant applicative feature since hydrophobic cement structures have i) longer
78 durability upon freezing-thawing cycles, as opposite to conventional porous and hydrophilic
79 composites which, after water absorption, tend to expand on freezing thus starting cracks within
80 the matrix; ii) self-cleaning ability; iii) resistance to paints/graffiti [14,15]. Also it has been
81 observed how hydrophobicity can be relevant to icephobicity [16,17]. At authors knowledge this
82 property of such composites has not been faced yet in published research.

83 Standard procedures for protecting cement structures are mainly based on impregnation and
84 coating methods, involving, therefore, only the modification of exterior layers and leaving a

85 hydrophilic bulk [15]. Specifically, silane or siloxane are mainly used for these applications
86 [18]. Recently, the addition of polymeric fibers to the paste mixture, combined to the use of a
87 hydrophobic coating, has been reported to reduce water penetration and to turn to hydrophobic
88 or over-hydrophobic nature this building material [17,19].

89 In this work, the effect of the TR grains addition to cement mortars has been investigated, with
90 specific reference to wetting properties, and more specifically to contact angle and absorption of
91 water drops. Tyre rubber was added to the mixtures formulation as partial and/or total
92 replacement of the conventional aggregate (sand). Aiming at affordable applications of this
93 process (addition of TR) we have tailored an addition to the cement paste without any use of
94 additive/chemical to improve adhesion. Since the material is modified in its whole mass, and no
95 coating is present on the surface, both the side surface and the inner (fracture) surface of the
96 mortars/specimens are of interest. Wetting properties are correlated to the micro-scale structure
97 (SEM) and the porosity of the specimens. Moreover, the mechanical properties of the
98 composites are also reported.

99 2. Materials and methods

100 2.1 Mortar specimens preparation

101 CEM II A-LL 42.5 R, a limestone Portland cement [20] provided by Buzzi Unicem S.p.A. was
102 used for the preparation of the cement composites. The main constituents are: 80-94% clinker,
103 6-20% limestone LL (<0.2% organic carbon), gypsum (0-5%), and minor additional
104 constituents; it shows high early resistance ($R_c(2 \text{ days}) > 25.0 \text{ MPa}$, $R_c(28 \text{ days}) > 47.0 \text{ MPa}$)
105 and Blaine specific surface area ranging $3100\text{-}4400 \text{ cm}^2/\text{g}$. Natural siliceous sand was provided
106 by Societ  Nouvelle du Littoral, Leucate, France with grains in the 0.08-2 mm size range
107 [21,22].

108 Mortar specimens were overall prepared using this type of cement, sand, tap water
109 (water/cement ratio kept constant at 0.5) and tyre rubber grains with particle size in the 0-2 mm
110 range. The samples were molded in the form of prisms (dimensions $40\times 40\times 160 \text{ mm}$) and 28
111 days water cured after demolding.

112 Tyre rubber was added to the mortars formulation as partial and/or total replacement of the
 113 conventional aggregate (sand). Table 1 and 2 report the aggregate and mortars composition.
 114 Sand replacement was made on volume basis rather than on weight basis due to the low specific
 115 weight of the lightweight materials under investigation. In order to tailor TR added mortars
 116 without the addition of chemicals to improve adhesion, we previously evaluated the maximum
 117 TR volume which could be incorporated into the mixture with an acceptable workability. Such a
 118 volume (500 cm³) was set as constant total volume of the aggregate. A reference, named Sand,
 119 prepared by using 500 cm³ of 0.5-2 mm sand, has been compared to the TR specimens. Total
 120 sand replacement was carried out with 100 % TR grains in the 0-0.5 mm size range (TR-small),
 121 100 % TR grains in the 0.5-2 mm size range (TR-large) and the last one with 50% TR grains in
 122 the 0-0.5 mm and 50% 0.5-2 mm (TR-mixed). Sand-TR sample was prepared by replacing 50%
 123 sand volume with TR grains in the 0-0.5 mm size range. A further conventional sand-based
 124 (normalized) mortar was prepared as control [21] and indicated as Normal.

125

sample	Type of aggregate	
Normal	Normalized sand	
Sand	Sieved sand (0.5-2 mm) 100%	
TR-small	Rubber Tyre (0-0.5 mm) 100%	
TR-large	Rubber Tyre (0.5-2 mm) 100%	
TR-mixed	TR (0-0.5 mm) 50%	TR (0.5-2 mm) 50%
Sand-TR	Sieved sand (0.5-2 mm) 50%	TR (0-0.5 mm) 50%

126

Table 1. Aggregates composition of the mortars.

127

128

129

130

131

132

133

Table 2. Mortars compositions.

sample	cement (g)	water (cm ³)	sand volume (cm ³)	TR volume (cm ³)
Normal	450	225	810	0
Sand	450	225	500	0
TR-small	450	225	0	500
TR-large	450	225	0	500
TR-mixed	450	225	0	500
Sand-TR	450	225	250	250

134

135

136

137 *2.2 SEM/ EDX analysis and porosimetric measurements*

138 Cement-based composites were characterized by scanning electron microscope (SEM) and
 139 energy dispersive X-ray (EDX) analysis. Specifically, in the case of SEM and EDX analysis,
 140 used to have magnified images and the elemental composition of the samples, an electron
 141 microscope FESEM-EDX Carl Zeiss Sigma 300 VP (Carl Zeiss Microscopy GmbH, Jena,
 142 Germany) was used. The samples were fixed on aluminum stubs and then sputtered with gold
 143 by the use of a Sputter Quorum Q150 (Quorum Technologies Ltd, East Sussex, UK).

144 Measurements of porosity % (parameter dependent on the total volume of the pores) were
 145 carried-out by Ultrapyc 1200e Automatic Gas Pycnometer (Quantachrome Instruments,
 146 Boynton Beach, FL, US). The apparatus utilises helium as inert gas which penetrates the finest
 147 pores of the material thus overcoming the influence of surface chemistry. Results are the
 148 average of three measurements performed onto three specimens of the same type.

149

150 *2.3 Contact Angle and water absorption measurements*

151 Contact angle measurements were performed by depositing water drops of 5 μ l (a number of 5
 152 drops per specimen) on the surface of the mortar specimens, both on the side surface and on the
 153 fracture (inner) one. A home-made system (Premier series dyno- lyte portable microscope and
 154 background cold lighting) allowed to record the evolution of the drop status in time, up to 100

155 s, at a frame rate of 30 frame per second. When the drop was not static (absorption took place)
156 acquired image sequences were analysed by the Image J software (National Institute of Health,
157 United States) in order to measure both variation of the contact angle and of the drop height
158 after release of the drop.

159

160 *2.4 Mechanical characterization*

161 Mechanical tests were carried-out by a MATEST system, Milan, Italy. Compression resistance
162 was carried out on samples deriving from flexural tests on 40×40×160 mm prisms after 28 days
163 curing [21-22]. Results are the average of the measurements performed on specimens of the
164 same type.

165 3. Theoretical background

166 In this section the terminology and the underlying theory about water contact angle and water
167 drops penetration is briefly presented as an introductory note to readers. The term wettability
168 refers to the ability of a surface to get wetted by a liquid, thus poor wettability refers to surfaces
169 that tend to repel that liquid. Hydrophobic refers to surfaces that repel water, while the
170 hydrophilic ones have favourable interactions with water. The critical parameter that is used to
171 evaluate the wettability of a solid surface is the contact angle of the liquid on the surface. In this
172 work the focus is only on water thus the term water contact angle (WCA) will be used
173 throughout. A surface is considered hydrophobic if the WCA is $> 90^\circ$; if $WCA < 90^\circ$ the surface
174 is considered as hydrophilic. If we consider a completely smooth and chemically homogeneous
175 surface (ideal), the chemistry of the solid surface is the only critical factor to determine its
176 wettability, which is evaluated by the Young equation:

$$177 \cos \vartheta = \frac{\gamma_{SG} - \gamma_{SL}}{\gamma_{LG}} \quad (1)$$

178]where ϑ is the contact angle (CA) of the liquid (water) droplet on the solid surface and γ_{SG} is
179 the solid-vapor interfacial energy, γ_{SL} is the solid-liquid interfacial energy and γ_{LG} is the liquid-

180 vapor interfacial energy[23]. For a given smooth surface, proper design of its chemistry is able
 181 to tailor the desired surface energy, i.e. the solid-vapor interfacial energy γ_{SG} , hence the desired
 182 θ [24]. If the solid surface is not smooth, or equivalently a certain roughness is present, the
 183 apparent contact angle differs from θ . Basically speaking for an inherent hydrophobic surface
 184 (low surface energy), an increase of surface roughness leads to an increase of hydrophobicity
 185 translated to higher apparent WCA. On the other hand, for an inherent hydrophilic surface an
 186 increase of surface roughness leads to an increase of hydrophilicity translated to lower apparent
 187 WCA [25-26]. This implies that the WCAs measured on the surfaces in this work, never ideally
 188 smooth, are apparent contact angles. However, it should be noted that the effect of roughness,
 189 for the composite materials under focus, can be considered at a first analysis less important than
 190 chemical non-homogeneity and porosity in driving wetting behaviour.

191 Regarding porosity, in the simple case of only one pore under the drop and with borders with a
 192 homogeneous chemistry (i.e. surface energy), the drop stands/is in equilibrium if the forces
 193 directed downwards (force due to Laplace pressure at the curved drop surface and gravitational
 194 force) are balanced by the meniscus tension on the pore perimeter (the one producing capillary
 195 pressure). The latter for fully hydrophobic materials is directed upwards, while for fully
 196 hydrophilic materials is directed downwards. In general [27-28], penetration occurs when net
 197 force F_{net} , given by the three terms (from left to right) expressing the force due to Laplace
 198 pressure, the gravitational force, and the force due to the meniscus on the pore perimeter is
 199 greater than zero that is:

$$200 \quad F_{net} = \frac{\pi\gamma d^2}{2R_d} + \rho g R_d (1 - \cos\theta) \frac{\pi d^2}{4} + \pi d \gamma \cos\theta > 0 \quad (2)$$

201 Here θ is the contact angle of the drop on the surface, d is the pore diameter, R_d the drop
 202 radius, γ is the surface tension of water, ρ is density of water, g is the gravitational acceleration,
 203 and $R_d(1 - \cos\theta)$ is the height of the drop. Thus in this simple case of only one and
 204 chemically homogeneous pore under the drop the parameters affecting motion of the drop are d ,
 205 R_d , θ .

206

207 4. Results and discussion

208 A picture of the specimens, on the left the Sand reference and on the right a TR mortar (TR-
209 small) is presented on the left of **figure 1**.

210 Characterization was performed both on the side and on the inner surface of the mortars. The
211 inner surface results from the fracture of the specimens occurring upon compression tests. A
212 magnified micrograph of a TR added sample can be appreciated on the right of figure 1. Side
213 and fracture surface are very different for both the reference sand samples and the TR added
214 ones. The side surface is almost homogeneously made of cement paste which, when fluid, can
215 better fill the space close to the mold surface. The fracture surface, instead, beside being
216 rougher, as a consequence of fracture, is characterized by a visible distribution of aggregates
217 (sand and /or TR grains) embedded in the cement paste.

218 Wetting results of the reference Sand sample are reported in figure 2 (side surface) and 3
219 (fracture surface). **Figure 2** diagrams report water contact angle (WCA) and drop height as a
220 function of time measured on the side surface in 5 different positions. A very different behavior
221 is observed on the various points: slow absorption in points 1 and 2, with the drop penetrating
222 below the surface in more than one minute; fast absorption in point 5, where a full penetration
223 occurs in few seconds; hydrophobic behavior in point 3 where the drop is completely stable
224 with a relatively high angle (120° , typical of hydrophobic solids such as Teflon [29]). When
225 penetration occurs, WCA generally follows the trend of the drop height: as the drop penetrates
226 (hence, as the height decreases) the contact angle also goes down, i.e. the drop spreads over the
227 surface. It means that the drop penetration in the composite proceeds in all the directions, both
228 orthogonal and parallel to the surface.

229 Results on the fracture surface of the reference sample are reported in **figure 3**. In this case a
230 very fast absorption is observed over all the tested points, with full penetration occurring even in
231 less than half second. Also in this case measurement of the WCA (not easy in this case due to
232 the macro-scale roughness of the surface and the very spread shape of the drop) follows the

233 trend of the drop height, thus a very fast spreading occurs together with the absorption. This
234 surface can be considered superhydrophilic [26] and fast absorbent. Almost identical results
235 (both on the surface and on the bulk) are observed on the standard N reference mortar (Normal).
236 It is reasonable to consider the behavior of the fracture surface as the one truly representative of
237 conventional mortars/concrete since representing a section of the artifacts with all the
238 components (cement paste and sand) and with an intrinsic porosity, i.e. not altered by the local
239 effect. It should be noted that as soon as the side surface undergoes wear, scratching or any
240 other damage, the inner material is disclosed and exposed to environment.

241 Wetting characterization results of TR mortars, specifically with small fraction TR size (TR-
242 small), are reported in **figure 4**. As described above, TR grains are added to the cement mixture
243 in total replacement of the sand volume. In this case both for the side surface (on the top) and
244 the fracture surface (on the bottom) only the drop height is diagramed, as the WCA trend is very
245 similar. It is absolutely interesting to appreciate that both on the side and on the fracture surface
246 the drop is stable on the surface (except a minimum height decrease in one point) for all the
247 observation time. The WCAs are nearly stable as reported in the diagram box; WCA_i are the
248 initial values for the points where a slight variation has been observed. WCA values are always
249 above 100 °, and in some cases even reaching 125°, on the side surface and above 90° on the
250 fracture one. This wetting behavior can be classified as from hydrophobic (WCA > 90°) to
251 overhydrophobic (WCA > 120°) and is that typical of the most hydrophobic among organic
252 polymers, such as PTFE (polytetrafluoroethylene) or PDMS (polydimethylsiloxane) [23,29].
253 Thus the presence of rubber prevails and makes ineffective the presence of the hydrophilic
254 cement regions in these mortars.

255 A comparison among this sample and the other TR- mortars (TR-large and TR-mixed) is
256 reported in **figure 5**, with the optical micrographs of the respective fracture surfaces at the top
257 and an histogram (at the bottom) reporting the water drop entry % (percent difference between
258 initial and final (at 100s) drop height). For every sample and every surface (with S as side, and F
259 as fracture) the water drop entry is averaged over the measurements of the five drops. Results
260 related to the Sand reference sample (presented in detail in figure 2) are here reported on the

261 average for comparison. As it can be appreciated all the TR-mortars present a pronounced
262 abatement (more than 80%) of the water absorption. Among these, the specimen fabricated with
263 smaller fraction rubber aggregates (TR-small) shows the best performance (more than 95%),
264 reasonably as a consequence of a denser distribution of hydrophobic sites on the surface.

265 Regarding this point it should be noted that under our conditions the contact area between water
266 and the sample surface is at least about 2 mm (as in the case of highly hydrophobic interaction,
267 as in the pictures of figure 4); the samples with larger grain size fraction (TR-large and TR-
268 mixed), since the total volume is constant, are also characterized by a lower number of particles.
269 Therefore, larger hydrophilic (cement paste) spaces are available where a slight access to water
270 is possible (optical micrographs in **figure 5** clarifies this aspect).

271 The possibility of using rubber and sand in the same mortar has been also tested with the aim to
272 combine the advantages of the standard sand aggregate and the features of rubber.

273 The behavior of mortars prepared by replacing 50% sand volume (Sand-TR-mortars) is reported
274 in **figure 6**. The optical micrograph on the top shows on the fracture surface distinguishable
275 sand grains together with the TR ones. Water absorption (water drop entry % in the diagram at
276 the bottom) is also significantly abated with respect to the reference samples, however it is
277 appreciably higher than the TR-mortars. Reasonably this less effective hydrophobization is due
278 to the halved volume of rubber, more than to the introduction of sand, which, is a hydrophilic
279 but non porous material.

280 In **figure 7** the inflection and compression resistance of these samples are reported as a function
281 of the specific weight. In particular, we find that total replacement of sand with TR grains
282 results in halving the specific weight with respect to the sand mortar. Moreover, the inflection
283 resistances and the compression resistances are sensitively lower than the reference sample.
284 Replacement of 50% sand volume with TR grains leads to an increase of the specific weight and
285 of the mechanical resistances with respect to the 100% sand replacement. Porosity % (by
286 Helium picnometer, sensitive to the total volume of the pores) of all these samples is reported in
287 **figure 8** diagram as a function of TR volume ratio. Three markers at 100% TR are related to the
288 three different TR grain size fractions. Independently of the rubber particle size fraction,

289 porosity turns out doubled with respect to the sand reference. Porosity of the TR-sand specimen
290 is also considerably higher than the reference. Overall, these results confirm the lightening and
291 pore-generating effect of the rubber aggregates, diffusively reported in literature, as described in
292 the introduction section. This can be considered an advantage in terms of building efficiency
293 [13]and suggests non structural and thermal insulating applications for these composites.

294 The porosity results can be explained by the SEM images reported in **figure 9**. Specifically,
295 rubber grains have an intrinsic micro-scale texture and porosity (“as received” rubber particle is
296 reported on the top). Further, as a consequence of the unfavorable adhesion between rubber and
297 cement paste, thoroughly discussed in introduction section, we also have verified the presence
298 of large voids around the rubber grains. The other images are those acquired on the sand
299 reference (middle) and on a TR-mortar (bottom). The length of the voids can reach the
300 dimensions of the TR grains (i.e. order of mm) and the width can be even 20-30 micron. This
301 effect has been also reported by other authors [30, 31]. EDX analysis have been performed to
302 have a detailed composition of the different regions of the composites. Basically, sand
303 composition is: C (4%), O (52%), Si (35%), Ca (2%); rubber composition is: C (25%), O (70%),
304 S (1.5%); cement paste composition is: C (5%), O (40%), Si (7%), Ca (40%), Fe (1%), Al (1%).
305 The porosity induced by rubber sites in this matrix could also increase water permeability [32].
306 However, these sites decrease the mean surface energy and our results show that this effect
307 prevails on the increased porosity in terms of mortar water penetration.

308 Penetration of water drops into hydrophobic pores is recently under study with the aim to
309 predict the behavior of such drops. Choi and Liang [33] have shown, with reference to eq. 2,
310 that onto fully hydrophobic surfaces with single or multiple pores with a set diameter the
311 smaller the drops (in the range 0.5-15 μ l) the less unfavorable the penetration is, since the
312 Laplace pressure can get larger than the meniscus force. For instance, 5 μ l drops can penetrate
313 into a fully hydrophobic material (polydimethylsiloxane, angle of about 110°) if the pores
314 diameter is greater than 500 μ m. In our case the surface is a composite matrix of hydrophilic
315 porous domains (cement paste) mixed to hydrophobic ones (rubber). Sand grains, when present,
316 represent hydrophilic but non porous domains. Thus these composites have multiple contact

317 angles: a hydrophobic contact angle (and meniscus angles) which is around 90 °, as it has been
318 measured on a flat sheet of tyre rubber, and a plurality of angle values in the hydrophilic field
319 (lower than 70°, also down to 5-10 °) relative to the cement paste and, eventually, sand grains.
320 Further, the pore diameter in the cement matrix spans in a very large range, from the nano- and
321 micro-scale scale [34, 35] to the macro-scale pore as those shown in the SEM) characterization.
322 Modeling this problem is therefore not straightforward and could be of high interest for next
323 studies. What we experimentally found is that with less than 50% surface area made of
324 hydrophobic matter (as it can be observed in optical images in figure 5) it is possible to get an
325 overall behavior of the composite material which is fully hydrophobic. A simplified scheme
326 sketching the status of a water drop on the surface of these composites is presented in **figure 10**.

327 Conclusions

328 In this work, it was evaluated the possibility of exploiting the low surface energy of tyre rubber
329 in order to induce protection in cement composites against penetration of water drops. Results
330 show that tyre rubber addition in cement mortars strongly abates penetration of small water
331 drops which goes from 100% in conventional specimens to 3-5 % in the rubberized ones.
332 Surface and bulk of these materials have very different structure and composition, nevertheless
333 they show a similar waterproof behavior. This means that the property exists in the whole
334 material and cannot be modified by eventual wear or damage events of the surface.

335 Maximum hydrophobic performances are found when the average size of the tyre rubber grains
336 size is finer and their total volume in the mixture is larger, i.e., after total replacement of the
337 conventional sand aggregate.

338 Interestingly, the hydrophobic character of the rubber, although increasing the porosity of the
339 mortars due to the limited adhesion to the cement paste, and in spite of the presence of
340 hydrophilic porous domains (cement) at the water-solid interface (more than 50% surface area),
341 prevails in nullifying the net force for penetration and stabilizing the deposited drops on the
342 surface.

343 Application in construction of tyre-rubber cement composites, already suggested for non-
344 structural and thermal insulating uses due to the lightweight and porous character, is now
345 strengthened by the hydrophobic behaviour here documented.

346 In particular, in light of such a property, they could find suitable applications in buildings as i)
347 plasters for outside walls and in general for vertical elements exposed to water flowing and
348 capillary rise, or ii) screeds for flat roofs and/or balconies. Other possible construction
349 applications, beside the already suggested sidewalks and playground pavements, are coatings
350 for tanks and gutters. Further work will be surely necessary in order to developing every
351 mentioned construction application, both in terms of specific standard characterizations and in
352 terms of eventual admixture optimization. However, these results first demonstrate a material
353 performance arising from the combination of rubber with a cement matrix. Finally, considering
354 the re-used origin of this material, it is easy understandable that tyre rubber-cement composites
355 are also cost-effective construction materials and in perfect agreement with the current policies
356 of environmental sustainability.

357

358 Acknowledgments

359 Rosa Di Mundo gratefully acknowledges the Future in Research Program of the Apulia Region
360 (Fondo di Sviluppo e Coesione 2007-2013 – APQ Ricerca Regione Puglia “Programma
361 regionale a sostegno della specializzazione intelligente e della sostenibilità sociale ed
362 ambientale”).

363 The authors acknowledge Adriano Boghetich and Ernesto Robertiello for the technical support
364 in specimens preparation, Marianna Gaudio and Priscilla Amodio for the assistance in data
365 analysis, Stefania Liuzzi and Pietro Stefanizzi for the porosity measurements.

366

367

References

- 370 [1] D. Lo Presti, Recycled Tyre Rubber modified bitumens for road asphalt mixtures: a
371 literature overview, *Constr. Build. Mater.* 49 (2010) 863-881.
- 372 [2] End of Life Tyres. [http://www.etrma.org/uploads/Modules/Documentsmanager/brochure-elt-](http://www.etrma.org/uploads/Modules/Documentsmanager/brochure-elt-2011-final.pdf)
373 [2011-final.pdf](http://www.etrma.org/uploads/Modules/Documentsmanager/brochure-elt-2011-final.pdf) , 2011 (accessed 08 October 2017).
- 374 [3] X. Shu, B. Huang, Recycling of waste tyre rubber in asphalt and portland cement concrete:
375 an overview, *Constr. Build. Mater.* 67 (2014) 217–224.
- 376 [4] M. Heitzman, design and construction of asphalt paving materials with crumb rubber
377 modifier, *Transport. Res. Record: J. transport Res. Board.* 1339 (1992) 1-8.
- 378 [5] B.Huang, G. Li, S.S. Pang, J. Eggers, Investigation into waste tyre rubber-filled concrete, *J.*
379 *Mater. Civ. Eng.* 16 (2004) 187-194.
- 380 [6] N. Segre, I. Joekes, Use of tyre rubber particles as addition to cement paste, *Cem. Concr*
381 *Res.* 30 (2000) 1421–1425.
- 382 [7] G. Li, M. A. Stubblefield, G. Garrick, J. Eggers, C. Abadie, B. Huang, Development of
383 waste tyre modified concrete, *Cem. Concr. Res.* 34 (2004) 2283–2289.
- 384 [8] G. Li, G. Garrick, J. Eggers, C. Abadie, M. A. Stubblefield, S.S. Pang, Waste tyre fiber
385 modified concrete, *Compos. Part B: Eng.* 35 (2004) 305-312
- 386 [9] B. I. Lee, L. Burnett, T. Miller, B. Postage, J. Cuneo, Tyre rubber/cement matrix composite,
387 *J. Mater. Sci. Lett.* 12 (1993) 967-968
- 388 [10] G. Li, Z. Wang, C. K. Y. Leung, S. Teng, J. Pan, W. Huang, E. Chen, Properties of
389 rubberised concrete modified by using silane coupling agent and carboxylated SBR, *J. Clean.*
390 *Prod.* 112 (2016) 797-807.
- 391 [11] N.N. Eldin, A.B. Senouci, Rubber-tyre practices as concrete aggregate, *J. Mater. Civ. Eng.*
392 5 (1993) 478–96.
- 393 [12] H. Zhu, T. Noresit, X. Zhang, Adding crumb rubber into exterior wall materials, *Waste*
394 *Manage Res.* 20 (2002) 407-13.
- 395 [13] V. Corinaldesi, A. Mazzoli, G. Moriconi, Mechanical behaviour and thermal conductivity
396 of mortars containing waste rubber particles, *Mater. Des.* 32 (2011) 1646-1650.

- 397 [14] E. Neto, S. Magina, A. Camoes, L. P. Cachim, A. Begonha, D. V. Evtuguin,
398 Characterization of concrete surface in relation to graffiti protection coatings, *Constr. Build.*
399 *Material*. 102 (2016) 435-444
- 400 [15] S. Weisheit, S.H. Unterberger, T. Bader, R. Lackner, Assessment of test methods for
401 characterizing the hydrophobic nature of surface-treated High Performance Concrete, *Constr.*
402 *Build. Mater*. 110 (2016) 145-153
- 403 [16] R. Ramachandran, M. Kozhukhova, K. Sobolev, M. Nosonovsky, Anti-Icing
404 Superhydrophobic Surfaces: Controlling Entropic Molecular Interactions to Design Novel
405 Icephobic Concrete, *Entropy* 18 (2016) 132.
- 406 [17] R. Ramachandran, K. Sobolev, M. Nosonovsky, Dynamics of Droplet Impact on
407 Hydrophobic/Icephobic Concrete with the Potential for Superhydrophobicity, *Langmuir*. 31
408 (2015) 1437-1444
- 409 [18] EN 1504-2, Products and systems for the protection and repair of concrete structures.
410 Definitions, requirements, quality control and evaluation of conformity in: Part 2: Surface
411 Materials and structures protection systems for concretes, BSI, Brussels, 2004.
- 412 [19] I. Flores- Vivian, V. Hejazi, M. I. Khozhukova, M. Nosonovsky, K. Sobolev, Self-
413 Assembling Particle-Siloxane Coatings for Superhydrophobic Concrete, *ACS Appl. Mater.*
414 *Interfaces*. 5 (2013) 13284-13294
- 415 [20] Cement Composition, Specifications and Conformity Criteria for Common Cements. EN
416 197-1, <http://store.uni.com/magento-1.4.0.1/index.php/en-197-1-2011.html>, 2011 (accessed 14
417 September 2011).
- 418 [21] Methods of Testing Cement-Part 1: Determination of Strength. EN 196-1,
419 <http://store.uni.com/magento-1.4.0.1/index.php/en-196-1-2016.html>, 2016 (accessed 27 April
420 2016).
- 421 [22] Cement, test methods, determination of strength. ISO 679, [http://store.uni.com/magento-](http://store.uni.com/magento-1.4.0.1/index.php/iso-679-2009.html)
422 [1.4.0.1/index.php/iso-679-2009.html](http://store.uni.com/magento-1.4.0.1/index.php/iso-679-2009.html), 2009 (accessed 24 April 2009).
- 423 [23] F. Palumbo, R. Di Mundo, Wettability: Significance and measurement, in: L. Sabbatini
424 (ed.) *Polymer Surface Characterization*, De Gruyter, Berlin, 2014, pp. 207-241.
- 425 [24] R. Di Mundo, F. Palumbo, R. d'Agostino, Influence of chemistry on wetting dynamics of
426 nanotextured hydrophobic surfaces, *Langmuir* 26.7 (2009): 196-5201.
- 427 [25] R. Di Mundo, F. Bottiglione, G. Carbone, Cassie state robustness of plasma generated
428 randomly nano-rough surfaces, *Appl. Surf. Sci.*, 16 (2014) 24-332.

429 [26] R. Di Mundo, R. D'Agostino, F. Palumbo, Long-Lasting Antifog Plasma Modification of
430 Transparent Plastics, *ACS Appl. Mater. Interfaces*. 6 (2014) 17059-17066.

431 [27] A. Marmur, Penetration and displacement in capillary systems of limited size, *Adv. Colloid*
432 *Interface Sci.* 39 (1992) 13–33.

433 [28] P. Yue, Y. Renardy, Spontaneous penetration of a non-wetting drop into an exposed pore,
434 *Phys. Fluids* 25 (5) (2013) 052104.

435 [29] N. Menga, R. Di Mundo, G. Carbone, Soft-Blasting of fluorinated Polymers: the easy way
436 to superhydrophobicity, *Mater Design*. 121 (2017) 414-420.

437 [30] A. Turatsinze, S. Bonnet, J. L. Granju, Mechanical characterisation of cement-based mortar
438 incorporating rubber aggregates from recycled worn tyres, *Build. Environ.* 40 (2005) 221-226.

439 [31] N. Segre, I. Joekes, Use of tyre rubber particles and addition, *Cem. Concr. Res.* 30 (2000)
440 1421–1425.

441 [32] D. M. Roy, P. W. Brown, D. Shi, B.E. Scheetz, W. May, Concrete microstructure porosity
442 and permeability, ARRB Group Lim, 1993.

443 [33] H. Choi, H. Liang, Wettability and spontaneous penetration of a water drop into
444 hydrophobic pores, *J. Colloid Interface Sci.* 477 (2016) 176–180.

445 [34] X. Chen, S. Wu, Influence of water-to-cement ratio and curing period on pore structure of
446 cement mortar, *Constr. Build. Mater.* 38 (2013) 804–812.

447 [35] R. Kumar, B. Bhattacharjee, Porosity, pore size distribution and in situ strength of concrete,
448 *Cem. Concr. Res.* 33 (2003) 155-164.

449

450

451

452

453

454

455

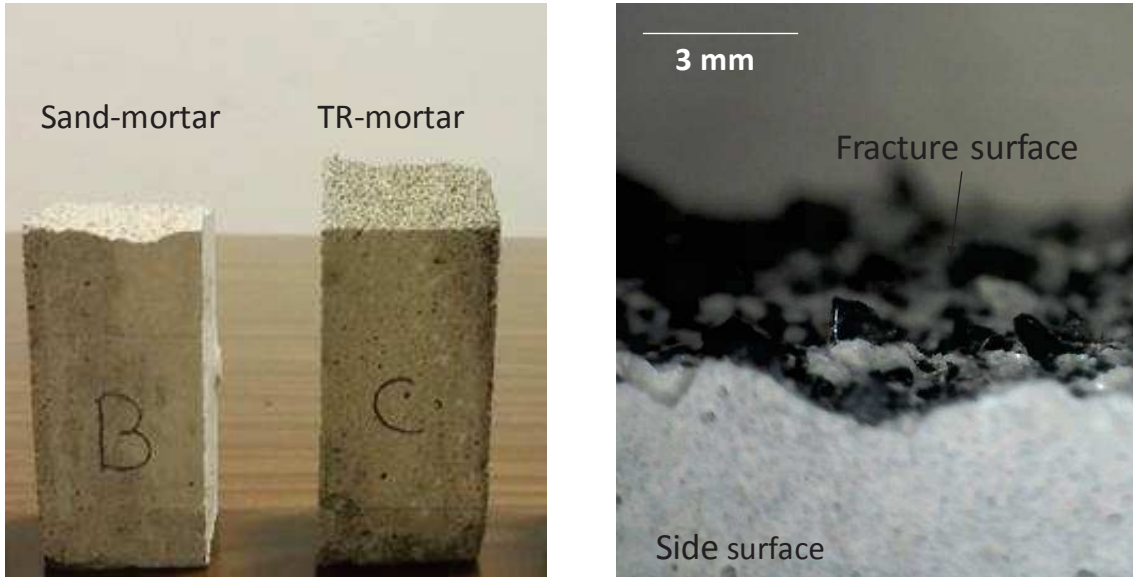
456

457

458

Figure 1

459



460

461 Figure 1. Picture of a sand based mortar (Sand reference) and TR added mortar (left);
462 micrograph of the side and fracture surface of a TR added mortar.

463

464

465

466

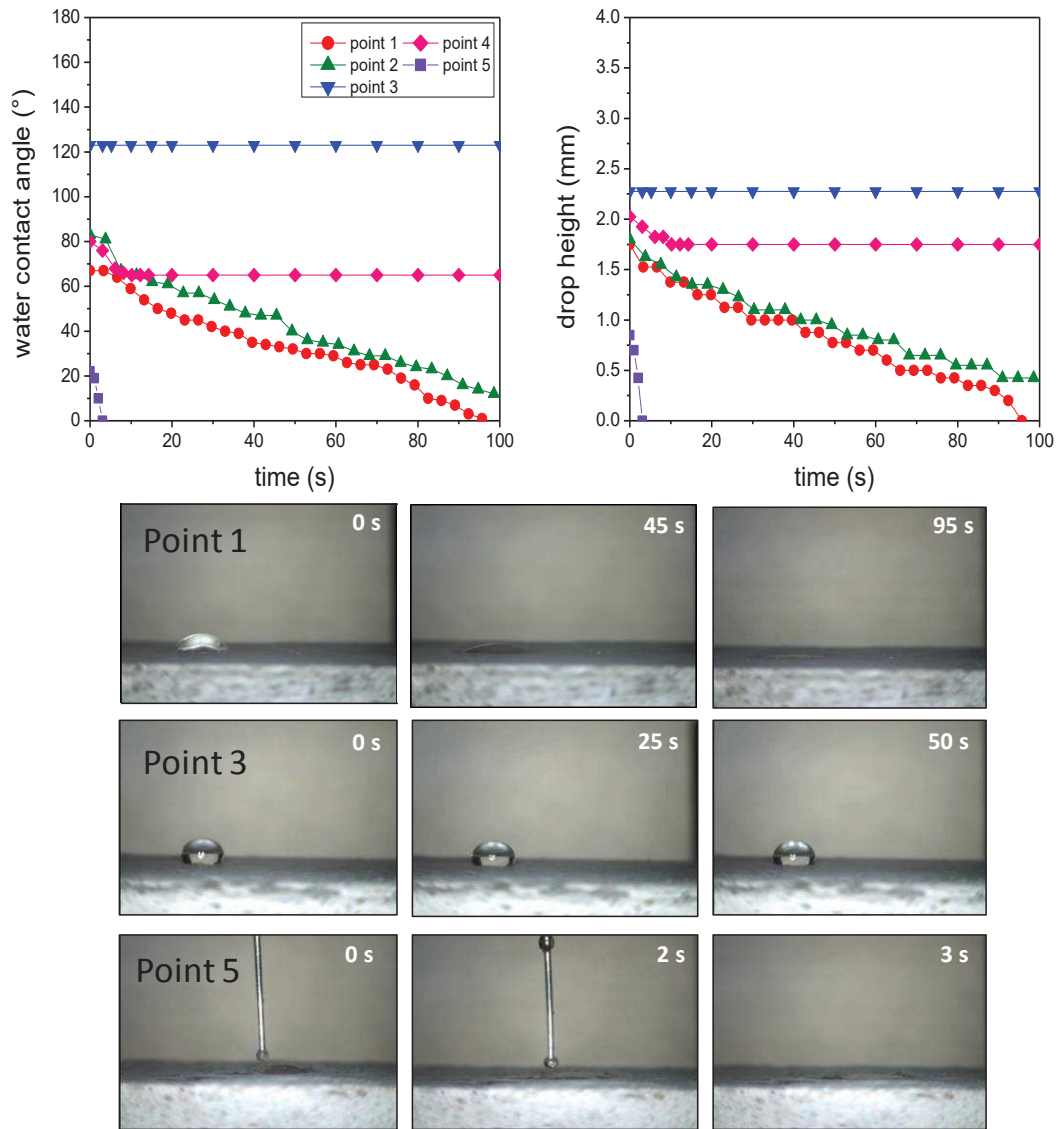
467

468

469

470

Figure 2



471

472

473

474

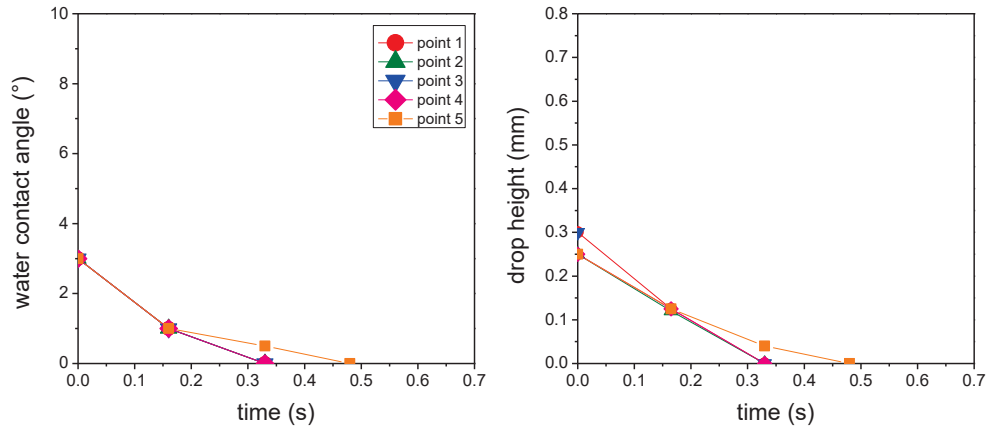
475

Figure 2: WCA and drop height as a function of time in the case of the side surface of the Sand reference mortar.

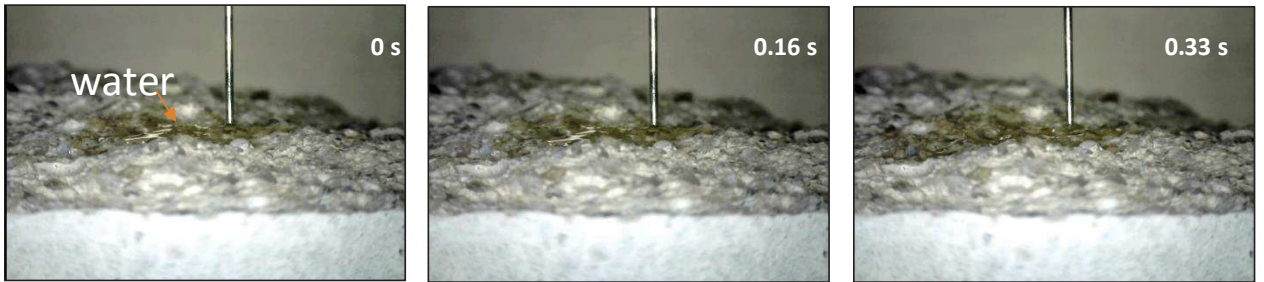
476

Figure 3

477



478



479 Figure 3: WCA and drop height as a function of time in the case of the fracture surface of the
480 Sand reference.

481

482

483

484

485

486

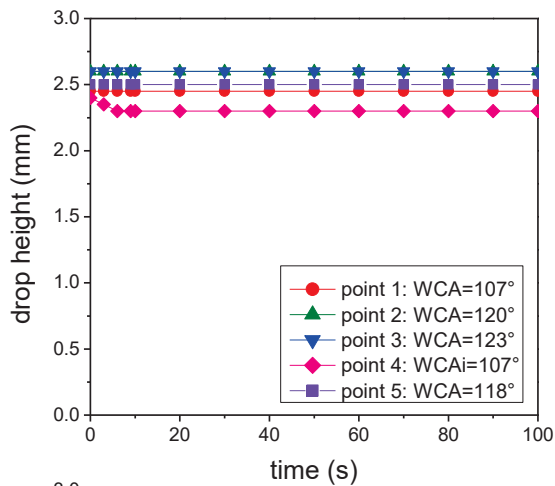
487

488

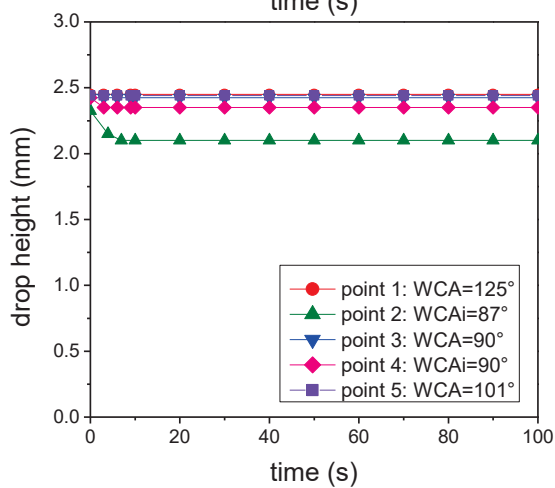
489

Figure 4

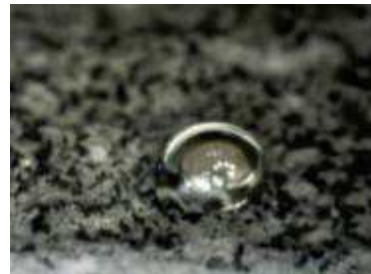
490



Point 3: WCA= 123°



Point 1: WCA= 125°



491

492

493

494

495

496

497

498

499

Figure 4: Drop height as a function of time in the case of the side surface (top) and of the fracture surface (bottom) of the TR-small sample. WCA values are reported in the diagrams legend. On the right, for each surface, a picture of the drop is reported related to one of the tested points.

500

501

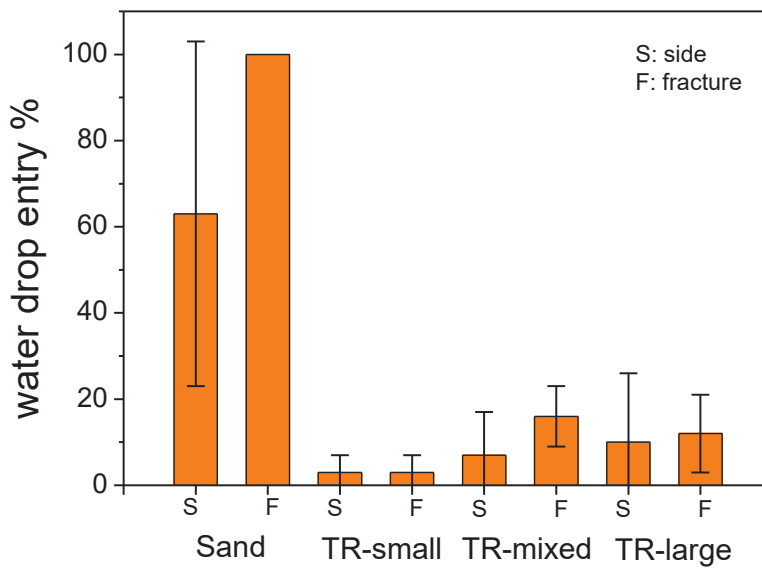
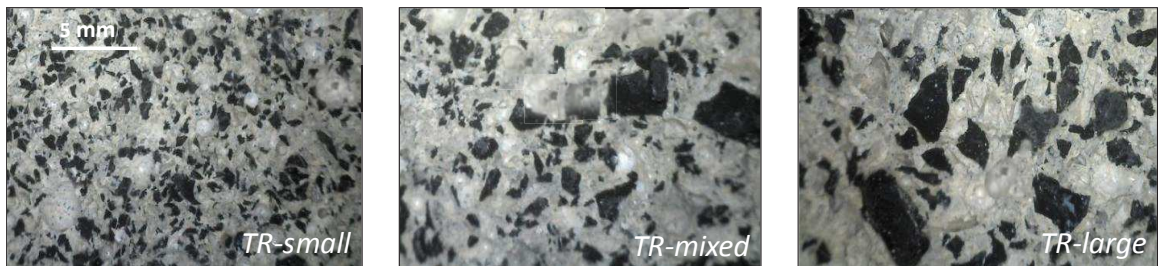
502

503

504

Figure 5

505



506

507

508

509

Figure 5: Water drop entry (%) in the case of the side and the fracture surfaces of the Sand reference, TR-small, TR-mixed, and TR-large samples. On the top: optical micrographs of the TR-samples.

510

511

512

513

514

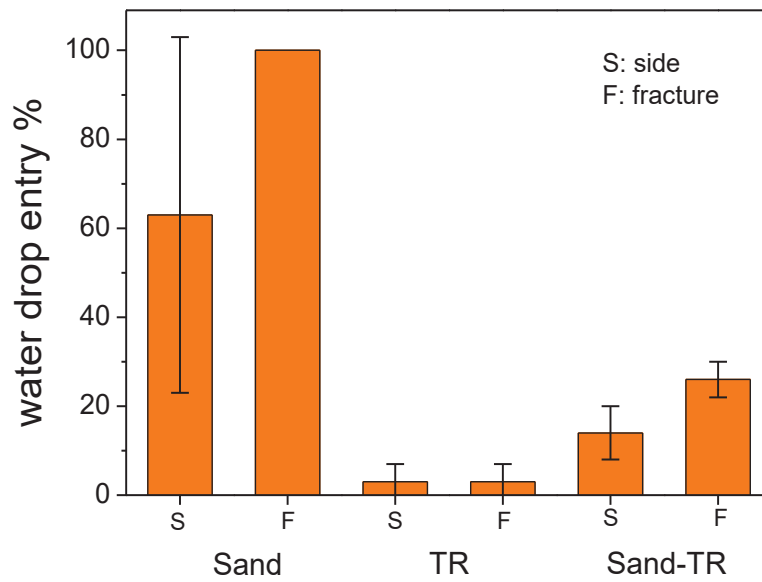
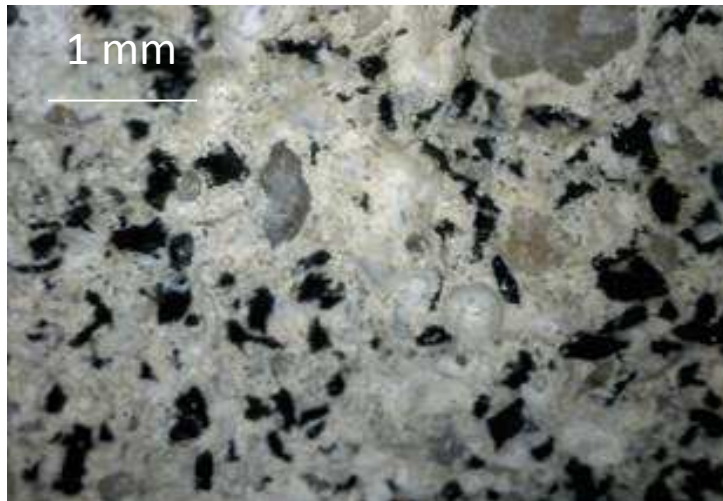
515

516

Figure 6

517

518



519

520

521

522

Figure 6: (top) Optical micrograph of the Sand-TR-sample. (bottom) Water drop entry (%) in the case of the side and fracture surfaces of the Sand reference, TR-small sample and Sand-TR sample.

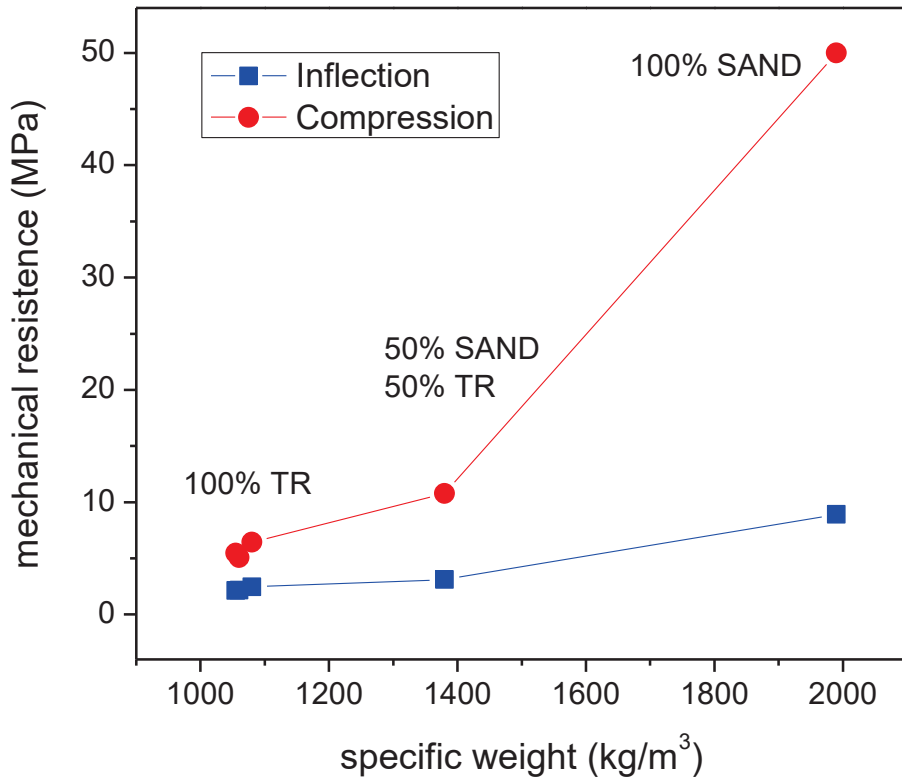
523

524

525

526

Figure 7



527

528

529

Figure 7: Mechanical resistances of the samples as a function of the specific weight.

530

531

532

533

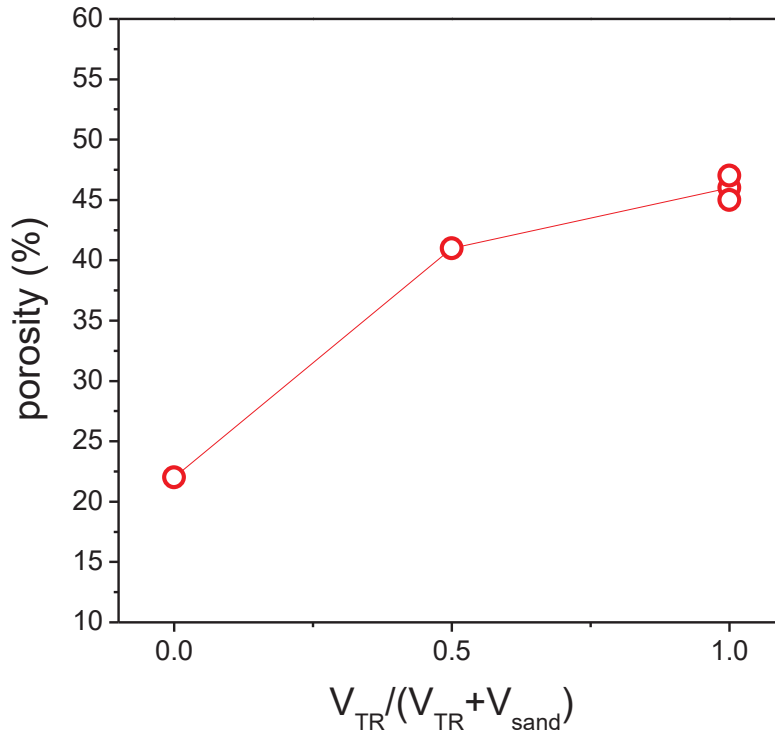
534

535

536

537

Figure 8



538

539 Figure 8: Porosity (%) of the samples as a function of TR volume ratio.

540

541

542

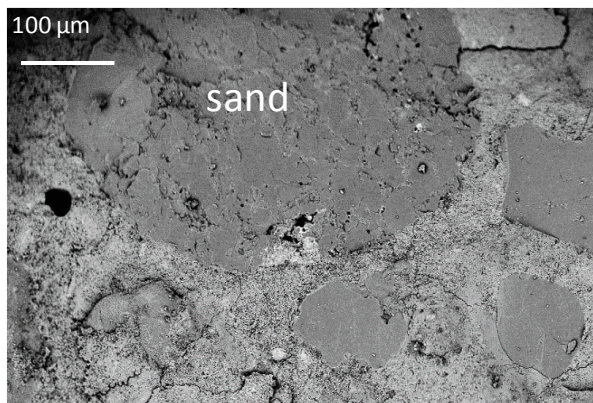
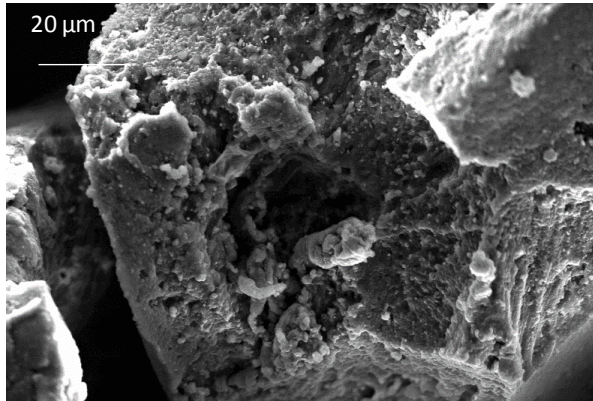
543

544

545

546

Figure 9



547

548

549

550

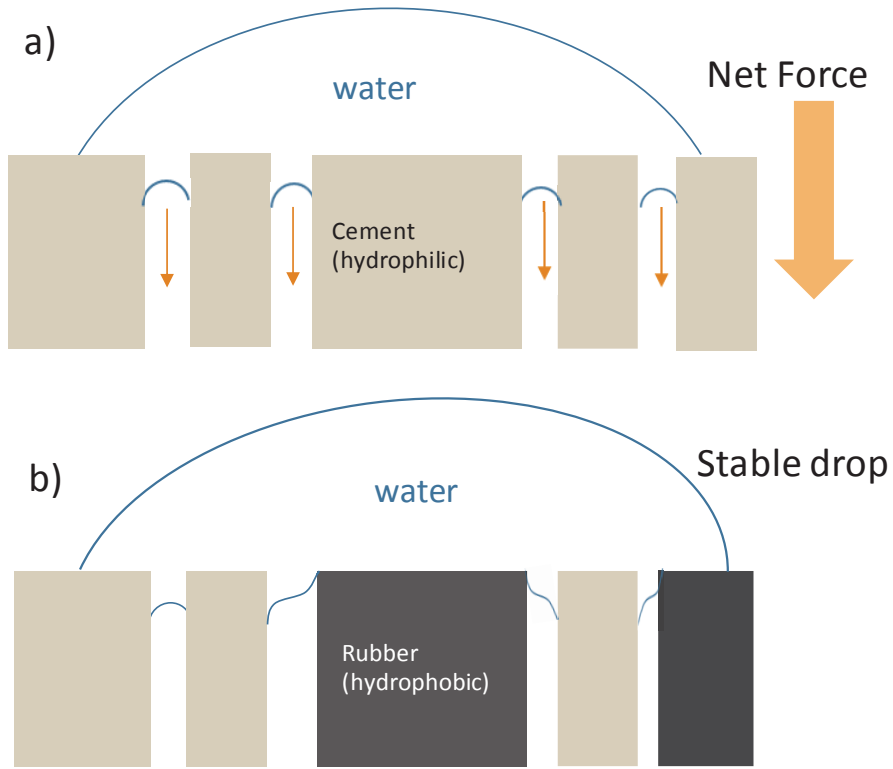
551

Figure 9: SEM images of a“as received” tyre rubber grain (top), Sand reference (middle), TR-small specimen (bottom)

552

553

Figure 10



554

555

556

557

558

Figure 10: Scheme sketching the drop on the surface of a) conventional (sand based) mortar with a surface uniquely made of high surface energy (hydrophilic) domains at various degree and b) a mortar containing tyre rubber grains, thus having a surface composed of very high surface energy (hydrophilic) and very low surface energy (hydrophobic) domains.

559

560

561

562

563